AMERICAN SOCIETY FOR MICROBIOLOGY | Molecular and Cellular Biology®

RESEARCH ARTICLE

α4 Coordinates Small Intestinal Epithelium Homeostasis by Regulating Stability of HuR

Hee Kyoung Chung,[a,b] Shelley R. Wang,[a,b] Lan Xiao,[a,b] Navneeta Rathor,[a,b] Douglas J. Turner,[a,b] Peixin Yang,[c] Myriam Gorospe,[d] Jaladanki N. Rao,[a,b] Jian-Ying Wang[a,b,e]

[a]Cell Biology Group, Department of Surgery, University of Maryland School of Medicine, Baltimore, Maryland, USA

[b]Baltimore Veterans Affairs Medical Center, Baltimore, Maryland, USA

[c]Department of Obstetrics, Gynecology and Reproductive Sciences, University of Maryland School of Medicine, Baltimore, Maryland, USA

[d]Laboratory of Genetics and Genomics, National Institute on Aging-IRP, NIH, Baltimore, Maryland, USA

[e]Department of Pathology, University of Maryland School of Medicine, Baltimore, Maryland, USA

ABSTRACT The mammalian intestinal epithelium is a rapidly self-renewing tissue in the body, and its homeostasis depends on a dynamic balance among proliferation, migration, apoptosis, and differentiation of intestinal epithelial cells (IECs). The protein phosphatase 2A (PP2A)-associated protein α4 controls the activity and specificity of serine/threonine phosphatases and is thus implicated in many cellular processes. Here, using a genetic approach, we investigated the mechanisms whereby α4 controls the homeostasis of the intestinal epithelium. In mice with ablated α4, the small intestinal mucosa exhibited crypt hyperplasia, villus shrinkage, defective differentiation of Paneth cells, and reduced IEC migration along the crypt-villus axis. The α4-deficient intestinal epithelium also displayed decreased expression of different intercellular junction proteins and abnormal epithelial permeability. In addition, α4 deficiency decreased the levels of the RNA-binding protein HuR in the mucosal tissue. In cultured IECs, ectopic overexpression of HuR in α4-deficient cells rescued the production of these intercellular junction proteins and restored the epithelial barrier function to a nearly normal level. Mechanistically, α4 silencing destabilized HuR through a process involving HuR phosphorylation by IκB kinase α, leading to ubiquitin-mediated proteolysis of HuR. These findings indicate that the critical impact of α4 upon the barrier function and homeostasis of the intestinal epithelium depends largely on its ability to regulate the stability of HuR.

KEYWORDS intestinal epithelial maturation, gut permeability, proliferation, differentiation, migration, conditional deletion

The mammalian intestinal epithelium is a vigorously self-renewing adult tissue in the body and functions as a physical barrier that separates mucosal tissues from luminal noxious substances and microbiota. Intestinal stem cells and amplified progenitor cells localized near the bases of the crypts drive this process and replicate perpetually, while the newly divided cells differentiate into all the mature cell types as they migrate up along the crypt-villus axis to replace lost cells (1, 2). The intestinal villi are the major functional compartment of the epithelium, which contains a number of differentiated and postmitotic cell types, such as absorptive enterocytes, mucus-secreting goblet cells, and hormone-secreting enteroendocrine cells (1, 3). Paneth cells, which secrete antibacterial peptides and growth factors, however, reside at the base of the crypt area of the intestinal mucosa. The maintenance of apical-basal polarity of intestinal epithelial cells (IECs) depends on a dynamic balance among multiple cellular activities, including proliferation, differentiation, migration, and apoptosis, that are tightly regulated by

Received 8 December 2017 **Returned for modification** 26 December 2017 **Accepted** 8 March 2018

Accepted manuscript posted online 19 March 2018

Citation Chung HK, Wang SR, Xiao L, Rathor N, Turner DJ, Yang P, Gorospe M, Rao JN, Wang J-Y. 2018. α4 coordinates small intestinal epithelium homeostasis by regulating stability of HuR. Mol Cell Biol 38:e00631-17. https://doi.org/10.1128/MCB.00631-17.

Address correspondence to Jaladanki N. Rao, rjaladanki@som.umaryland.edu, or Jian-Ying Wang, jywang@som.umaryland.edu.

distinct signaling networks (4, 5). Disruption of the integrity of the intestinal epithelium occurs commonly in various critical pathological conditions, leading to the translocation of luminal toxic substances and bacteria to the bloodstream and, in some instances, multiple-organ dysfunction syndromes and death (6, 7).

The α4 protein, encoded by the human *IgBP1* gene, was initially identified as an immunoglobulin-binding protein in mammalian B and T lymphocytes and was later found to be broadly expressed (8). Subsequent evidence indicated that α4 is an essential gene in all cell types and organisms in which it has been studied and is crucial for phosphatase biology (9, 10). α4 is a key regulator of protein phosphatase 2A (PP2A), PP4, and PP6, which collectively account for most cellular serine/threonine phosphatase activity (11). The catalytic subunit of PP2A is one of the most conserved enzymes in eukaryotic cells and has been involved in many aspects of cell functions and pathologies by dephosphorylating serine and threonine without significant influence from the flanking residues in the substrate (12, 13). Unlike those of kinases, the activities and specificities of serine/threonine phosphatases are primarily controlled by their associated proteins (14). Binding of α4 to PP2A displaces the scaffolding (PP2Aa and PR65) and regulatory (PP2Ab) subunits that constitute the PP2A heterotrimeric complex and modulate both enzymatic activity and substrate specificity (10, 11, 15). As a noncatalytic subunit of PP2A, α4 plays an important role in the regulation of cell spreading, migration, apoptosis, and proliferation (9, 12, 13). The levels of α4 increase significantly in several cancers and transformed cells (10, 12), whereas α4 depletion induces apoptosis in murine cells (9) and alters proliferation and migration in cancer cells (12, 13). To date, however, the physiological role of α4 in the control of intestinal epithelium homeostasis has not been established.

Studies using tissue-specific gene knockout and transgenic approaches in mice have provided powerful genetic evidence for physiological roles of various cellular factors in the development and homeostasis of the intestinal epithelium, although the results in mice, in some cases, contradict conventional predictions based on previous studies in cultured cells (16, 17). For example, despite the proliferative influence of the small GTPase Cdc42 (18), its targeted deletion in IECs resulted in gross hyperplasia of the intestinal epithelium, crypt enlargement, microvillus inclusion, and increased gut permeability (19). Similarly, intestinal epithelium-specific deletion of the RNA-binding protein (RBP) HuR (ELAVL1), which promotes division in cultured cells (20), caused significant mucosal atrophy in the small intestine and decreased the regenerative potential of crypt progenitors after injury (5, 21). In other cases, mouse studies and cultured cell studies agree; for example, expression of the microRNA miR-222 inhibits growth of cultured IECs and delays the repair of damaged mucosa in mice (22). Here, we report that α4 plays an essential role in the maturation of the intestinal mucosa and the integrity of the intestinal barrier, at least in part by maintaining HuR stability.

RESULTS

Expression pattern of α4 in the intestinal epithelium in response to stress. To begin to investigate the involvement of α4 in intestinal mucosal homeostasis and pathologies, the basal levels of α4 protein were examined in three different lines of cultured IECs, i.e., undifferentiated IEC-6, differentiated IEC-Cdx2L1, and Caco-2 cells, and in the intestinal mucosal tissue. All three lines of cultured IECs expressed α4 and its binding partners PP2A and β-PIX (p21-activated kinase-interacting exchange factor) (Fig. 1A, top), although the levels of α4, PP2A, and β-PIX in IEC-Cdx2L1 and Caco-2 cells were higher than those observed in IEC-6 cells. To examine the association of α4 with PP2A and β-PIX, whole-cell lysates were incubated with an antibody that recognized α4; following immunoprecipitation (IP), the levels of PP2A and β-PIX in the IP materials were examined by Western blotting. As shown in Fig. 1A (bottom), α4 physically interacted with PP2A and β-PIX and formed an α4/PP2A/β-PIX complex in cultured IECs. In control IP reactions, IgG did not immunoprecipitate either PP2A or β-PIX (data not shown). Immunostaining of the mucosa of the small intestine in mice showed that α4 was expressed in both the villous area and the crypt region (Fig. 1B, left). α4 was also

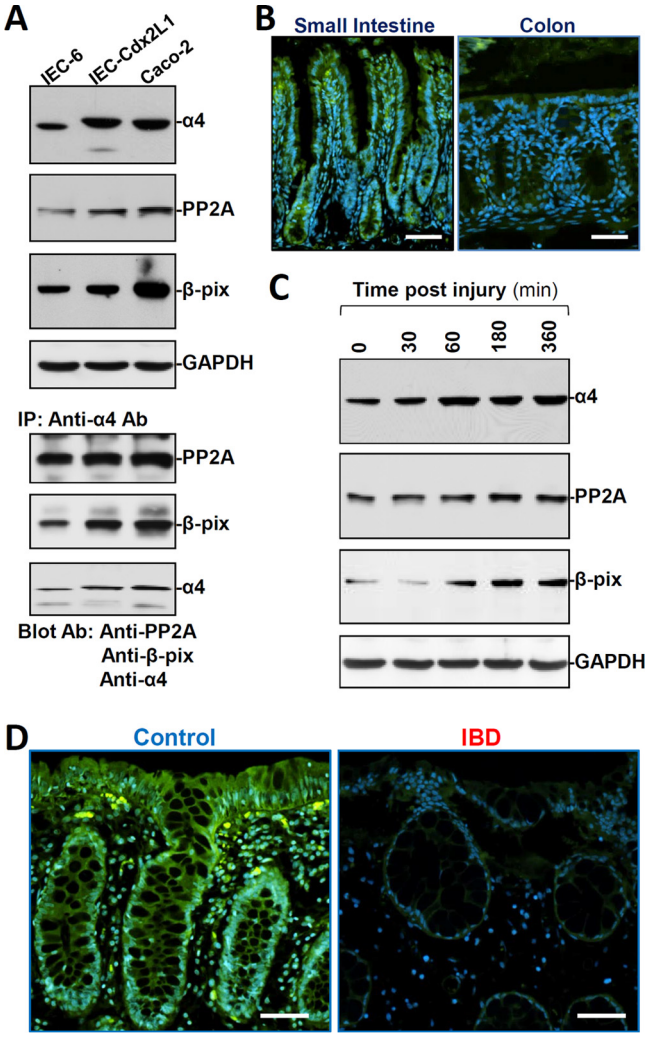

FIG 1 Expression levels of α4 in the intestinal epithelium with or without pathological stress. (A) Representative immunoblots of α4, PP2A, and β-PIX proteins (top) and their interaction (bottom) in different lines of cultured IECs. In studies examining protein-protein interactions, whole-cell lysates (400 μg) were immunoprecipitated by using an antibody (Ab) that recognizes α4, and the levels of PP2A, β-PIX, and α4 in the products of the IP reactions were examined by Western blotting. (B) Immunostaining of α4 (green) in mouse mucosal tissues from the small intestine and colon. Scale bars, 50 μm. (C) Changes in the levels of α4, PP2A, and β-PIX after wounding in cultured differentiated IEC-Cdx2L1 cells. After the cells were grown to confluence, epithelial repair was induced by removing part of the monolayer. The levels of α4, PP2A, and β-PIX were examined at different times after wounding. (D) Immunostaining of α4 in human intestinal mucosal tissues from control individuals (without mucosal erosions/inflammation) and from patients with IBD. The experiments were repeated in samples obtained from four patients with IBD or control individuals and showed similar results. Scale bars, 50 μm.

expressed in the colonic mucosa, although the basal abundance was lower in the colon than in the small intestine (Fig. 1B, right).

To examine changes in α4 expression in response to the stressful environment in IECs, we employed a previously described (5) *in vitro* repair model that mimics the early cell division-independent stage of intestinal epithelial restitution. As reported previously (5, 23), epithelial restitution occurred rapidly after wounding, as revealed by a significant increase in cell migration over the wounded area by 6 h (data not shown). Interestingly, the levels of α4 protein increased remarkably 1 h after wounding and remained elevated for an additional 5 h (Fig. 1C). As expected, the increase in α4 levels in migrating cells was associated with an increase in the cellular abundance of PP2A and β-PIX after wounding. Moreover, the colonic mucosal tissues obtained from patients with inflammatory bowel disease (IBD) exhibited levels of α4 significantly

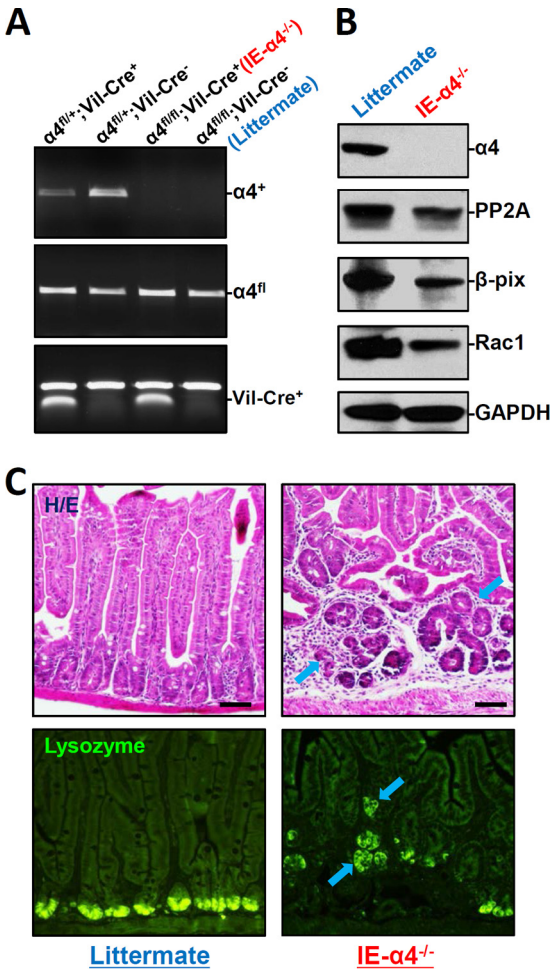

FIG 2 *α4* deletion in IECs disrupts mucosal maturation in the small intestine. (A) PCR analysis of genomic DNA from the small intestinal mucosa indicating floxed, α4 deletion, and Vil-Cre bands in mice with different genotypes. (B) Immunoblots of α4, PP2A, Rac1, and β-PIX proteins in the small intestinal mucosa obtained from controls (littermate) and intestinal epithelial tissue-specific α4 knockout (IE-$\alpha4^{-/-}$) mice. (C) Photomicrographs of hematoxylin and eosin (H/E) (top) and immunostaining of lysozyme (bottom), shown as in green, in the small intestine. Scale bars, 50 μm.

lower than those in control patients (without mucosal injury or inflammation), as measured by immunostaining analysis (Fig. 1D). The decreased abundance of mucosal α4 in patients with IBD was associated with delayed repair of damaged mucosa and gut barrier dysfunction, as evidenced by the decreased levels of the tight junction protein occludin (OCLN) (data not shown), as previously reported (4). These results suggest the potential importance of α4 in maintaining the integrity of the intestinal epithelium and the implication of its reduction in pathogenesis of mucosal inflammation/erosions and delayed repair.

A mouse model of α4 deficiency in the intestinal epithelium. To investigate the *in vivo* function of α4 in the mammalian intestinal epithelium, mice bearing a specific deletion of α4 in the intestinal epithelium (IE-$\alpha4^{-/-}$ mice) were generated by crossing villin (Vil)-Cre-expressing mice with $\alpha4^{flox/flox}$ ($\alpha4^{fl/fl}$) mice (see Fig. S1A in the supplemental material) (21, 24). $\alpha4^{fl/fl}$ mice had been produced previously (24) via standard gene targeting in embryonic stem cells and contained a fully functional α4 allele. Heterozygous IE-$\alpha4^{fl/+}$ mice appeared phenotypically normal and were subsequently intercrossed for the generation of homozygous IE-$\alpha4^{-/-}$ mice. As shown in Fig. 2A, homozygous IE-$\alpha4^{-/-}$ mice lacked the wild-type *α4* gene in the intestinal mucosa, and the levels of *α4* mRNA (see Fig. S1B in the supplemental material) and protein (Fig. 2B)

in the intestinal mucosa were undetectable in IE-$\alpha4^{-/-}$ mice. On the other hand, levels of *α4* mRNA were normal in off-target tissues, such as stomach, heart, liver, spleen, and kidney (see Fig. S1C in the supplemental material). We did not detect a compensatory increase in expression of PP2A, β-PIX, or Rac1 (a member of the GTPase family) in the IE-$\alpha4^{-/-}$ mice. In contrast, the levels of PP2A, β-PIX, and Rac1 proteins in the α4-deficient epithelium decreased by ~39%, ~61%, and ~40% ($n = 4$; $P < 0.05$), respectively. Littermate ($\alpha4^{fl/fl}$-Cre$^-$) and IE-$\alpha4^{-/-}$ mice were born in normal Mendelian ratios, but the IE-$\alpha4^{-/-}$ mice were significantly smaller and weighed less than the littermate controls (see Fig. S2A and B in the supplemental material). Gross analysis of gastrointestinal (GI) morphology revealed that the GI tract was shorter and thinner in IE-$\alpha4^{-/-}$ mice than in littermates (see Fig. S2C in the supplemental material); there was no intestinal bleeding or diarrhea in either mouse. These findings show that the IE-$\alpha4^{-/-}$ mouse is a suitable gene-targeting model of α4 deficiency in the intestinal epithelium.

α4 deletion disrupts mucosal maturation and homeostasis of the small intestine. A prominent phenotype observed in IE-$\alpha4^{-/-}$ mice was the inhibition of small intestinal mucosal maturation, as indicated by abnormal histological features, such as crypt hyperplasia and villous shrinkage (Fig. 2C, top). The architecture of the mucosal epithelium in the small intestine in IE-$\alpha4^{-/-}$ mice was markedly disrupted: the crypt dimensions increased, with a concomitant rise in the proliferation of connective tissue in the crypt area, whereas the length of the villus decreased. To examine if the localization or differentiation of Paneth cells was altered in the α4-knockout mouse, lysozyme-immunostaining assays were performed. As shown in Fig. 2C (bottom), lysozyme-positive cells, normally located at the base of the crypt, were displaced to the tops of crypts or the villous area and were fewer in the small intestinal mucosa in IE-$\alpha4^{-/-}$ mice. Comparison of the intestinal mucosa in IE-$\alpha4^{-/-}$ mice with that in control littermates revealed no changes in the abundance of alkaline phosphatase or sucrose isomaltase (two brush border membrane proteins), as determined by immunohistochemistry, and no changes in the numbers of goblet cells in the small intestinal mucosa, as examined by alcian blue staining (see Fig. S3 in the supplemental material).

As shown in Fig. 3A, the majority of crypt cells in the small intestinal mucosa were actively cycling, as assessed by measuring bromodeoxyuridine (BrdU) incorporation in IE-$\alpha4^{-/-}$ mice and littermates. However, the population of proliferating crypt cells increased significantly in the small intestinal mucosa of IE-$\alpha4^{-/-}$ mice relative to littermates (Fig. 3B). The levels of the cell proliferation marker protein PCNA were also increased by ~2.2-fold ($n = 3$; $P < 0.05$) in IE-$\alpha4^{-/-}$ mice (Fig. 3C), and the α4-deficient epithelium of the small intestine exhibited a deeper crypt and shorter villus, resulting in a decrease in the villus/crypt ratio (Fig. 3D). We also examined the influence of α4 deficiency on intestinal epithelial cell migration by using the BrdU chase method. In this study, mice examined at 1, 4, 16, and 24 h after BrdU pulse-labeling showed that BrdU-retaining cells displayed lower crypt-to-villus migration rates in IE-$\alpha4^{-/-}$ mice than in control mice (see Fig. S4A in the supplemental material). Additionally, α4 deletion induced apoptosis in the intestinal epithelium, with higher cell death in the mucosa of the small intestine in IE-$\alpha4^{-/-}$ mice, as assessed by terminal deoxynucleotidyltransferase-mediated dUTP-biotin nick end labeling (TUNEL) staining (see Fig. S4B and C in the supplemental material). Together, these findings indicate that α4 is essential for the maturation of the intestinal mucosa and the maintenance of homeostasis by modulating the proliferation, differentiation, migration, and apoptosis of IECs.

α4 deficiency impairs the epithelial barrier function by downregulating HuR. To gain a deeper understanding of the abnormalities of IE-$\alpha4^{-/-}$ mice, analysis of gut permeability and expression of intercellular junction (IJ) proteins revealed that the α4-deficient epithelium failed to maintain a proper barrier function. As shown in Fig. 4A, the levels of the tight junction (TJ) proteins claudin-1, claudin-3, and ZO-1, as well as the levels of the adherens junction (AJ) protein E-cadherin, in the α4-deficient intestinal tissue decreased by ~47%, ~98%, ~66%, and ~90% ($n = 4$; $P < 0.05$),

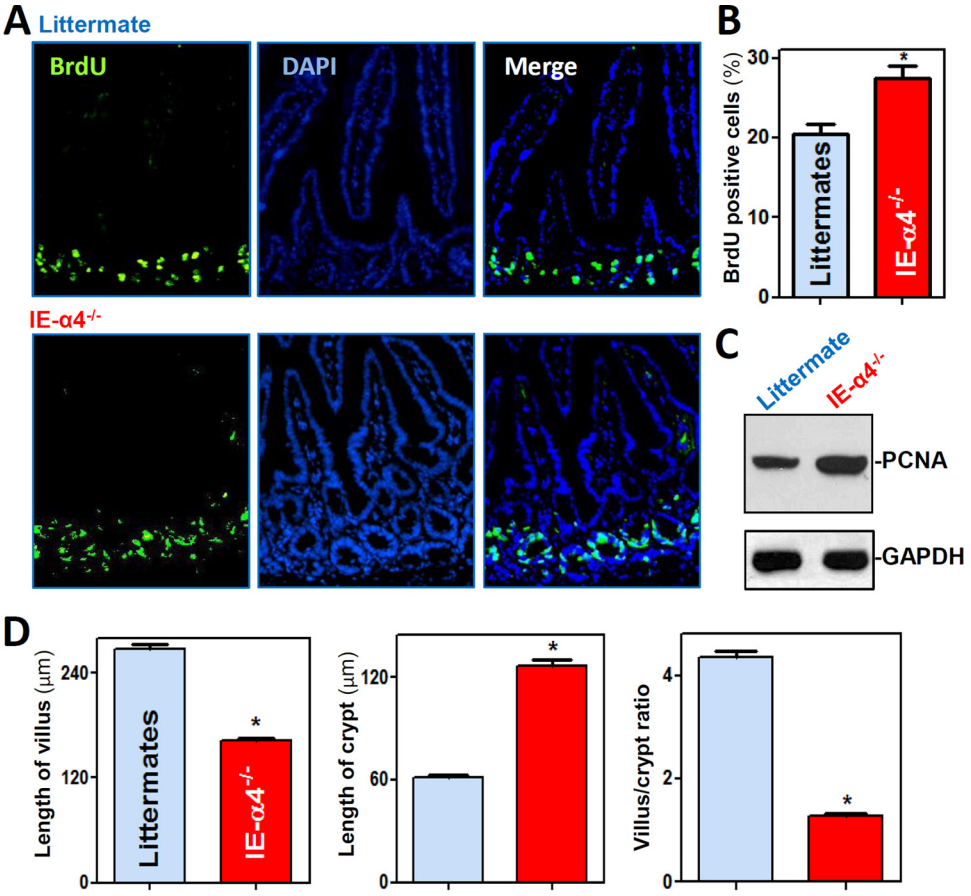

FIG 3 $\alpha 4$ deletion increases crypt depth but decreases villus height in the small intestine. (A) Proliferating cells in small intestinal crypts as measured by BrdU labeling (shown as green; S phase) in littermate (top) and IE-$\alpha 4^{-/-}$ (bottom) mice. The mucosa was harvested 30 min after the mice were injected with BrdU. (B) Summarized data for BrdU-positive cells in the mucosa shown in panel A ($n = 6$). *, $P < 0.05$ compared with littermates. (C) Levels of PCNA protein in the small intestinal mucosa. The error bars indicate SEM. (D) Changes in the lengths of villi (left) and crypts (middle) and villus/crypt ratios (right) of the small intestinal mucosa. *, $P < 0.05$ compared with littermates.

respectively. In contrast, there were no significant changes in the expression levels of the TJ protein occludin or the AJ protein β-catenin (data not shown) in IE-$\alpha 4^{-/-}$ mice. Notably, the mRNAs encoding claudin-1, claudin-3, ZO-1, and E-cadherin have U-rich, AU-rich, and other HuR-binding sites in their 3′ untranslated regions (UTRs) (25). Moreover, gut permeability to fluorescein isothiocyanate (FITC)-dextran increased significantly in IE-$\alpha 4^{-/-}$ mice compared with control mice (Fig. 4B). Interestingly, targeted deletion of $\alpha 4$ in IECs specifically decreased the levels of the RBP HuR by ~95% ($n = 4$; $P < 0.05$) in the mucosa of the small intestine, but it did not alter mucosal CUG-binding protein 1 (CUGBP1) levels (Fig. 4A).

Since HuR is a major regulator of IJ expression and gut permeability (26, 27), we hypothesized that $\alpha 4$ deletion in IECs might elicit epithelial barrier dysfunction by reducing HuR levels. To test this possibility, we silenced $\alpha 4$ in cultured IECs and examined changes in the abundances of HuR, various TJ proteins, and E-cadherin. Interestingly, decreasing $\alpha 4$ levels by transfecting differentiated IEC-Cdx2L1 cells with small interfering RNA (siRNA) targeting $\alpha 4$ mRNA (si$\alpha 4$) also lowered cellular HuR levels, associated with reduced production of claudin-3, ZO-1, and E-cadherin (Fig. 4C), similar to what was observed in IE-$\alpha 4^{-/-}$ mice; $\alpha 4$ silencing in cultured IECs did not alter occludin or CUGBP1 levels. Moreover, $\alpha 4$ silencing disrupted epithelial barrier function in these cells, as evidenced by a decrease in transepithelial electrical resistance (TEER) values and an increase in the levels of paracellular flux of FITC-dextran (Fig. 4D, bottom).

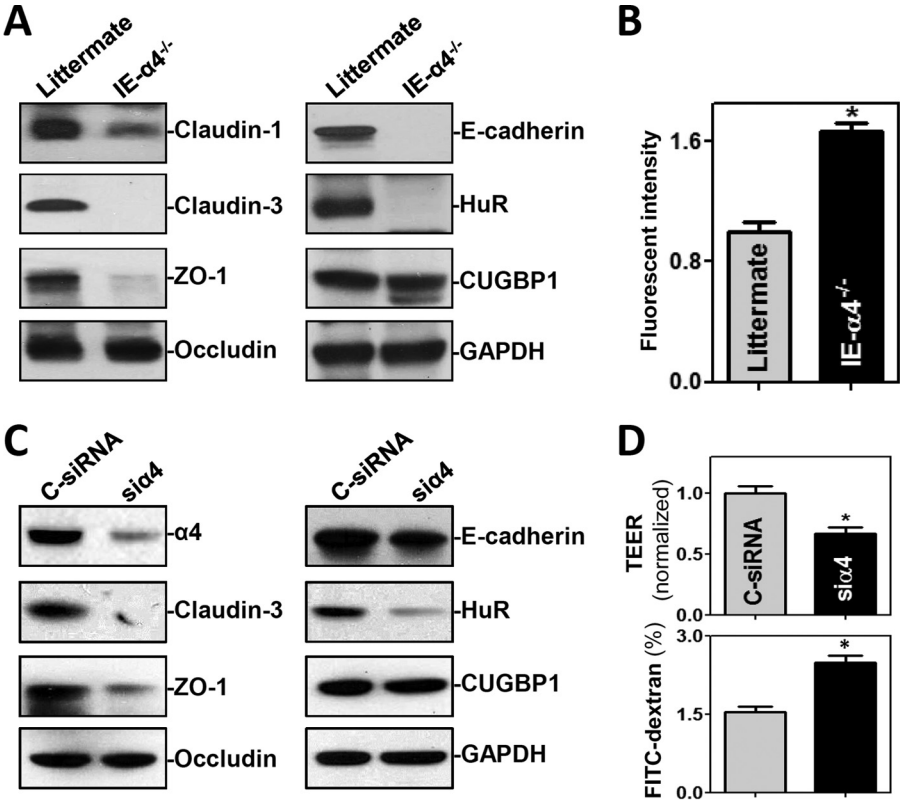

FIG 4 α4 knockout disrupts the intestinal epithelial barrier function *in vivo* and *in vitro*. (A) Immunoblots of the TJs claudin-1, claudin-3, ZO-1, and occludin; the AJ E-cadherin; and the RBPs HuR and CUGBP1 in the small intestinal mucosa obtained from littermate and IE-HuR$^{-/-}$ mice. (B) Changes in gut permeability in mice shown in panel A. FITC-dextran was given orally, and blood samples were collected 4 h thereafter for measurement. The values are means and SEM of data from 5 animals. *, $P < 0.05$ compared with littermates. (C) Immunoblots of intercellular junction proteins and RBPs in cultured IECs. Differentiated IEC-Cdx2L1 cells were transfected with C-siRNA or siα4, and cell lysates were harvested 48 h thereafter. (D) Epithelial barrier function as indicated by changes in TEER and FITC-dextran paracellular permeability in the cells shown in panel C. TEER assays were performed on 12-mm Transwell filters; paracellular permeability was assayed by using the membrane-impermeable trace molecule FITC-dextran, which was added to the medium in the insert part of the Transwell plate. The values are means and SEM of data from six samples. *, $P < 0.05$ compared with C-siRNA.

To investigate if increasing the levels of HuR rescued the epithelial barrier function in α4-silenced cells, we cotransfected cells with siα4 and a plasmid vector that expresses HuR. As shown in Fig. 5A, the decreases in claudin-1, claudin-3, ZO-1, and E-cadherin levels elicited by α4 silencing were largely rescued by HuR overexpression. Accordingly, the epithelial barrier function was also restored by ectopic overexpression of HuR in α4-silenced cells (Fig. 5B), with cellular TEER values and FITC-dextran flux indistinguishable from those in cells transfected with control siRNA (C-siRNA). These findings indicate that α4 regulates the epithelial barrier function in large part by enhancing HuR production in the intestinal epithelium.

α4 silencing destabilizes HuR through IKKα-dependent HuR phosphorylation and subsequent ubiquitin-mediated proteolysis. Interestingly, α4 silencing enhanced the degradation of HuR protein in IECs. As shown in Fig. 6A and B, the levels of HuR protein in the α4-silenced population of cells decreased gradually with the time after administration of cycloheximide (CHX), although there were no changes in HuR abundance in control cells treated with CHX. In addition, α4 silencing did not affect *HuR* mRNA levels or stability (see Fig. S5 in the supplemental material), indicating that the decrease in HuR levels in α4-deficient cells resulted primarily from reduced stability of the HuR protein rather than inhibition of *HuR* gene transcription or reduced *HuR* mRNA stability. Because the HuR protein is subject to ubiquitin-dependent degradation that

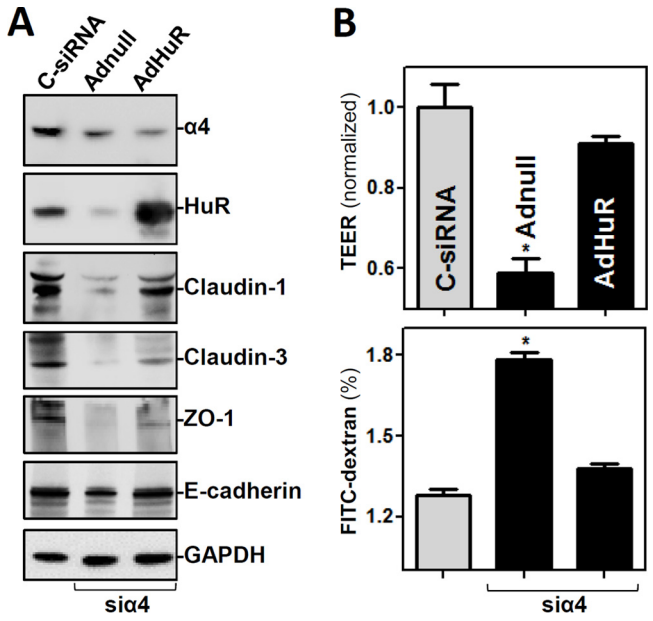

FIG 5 Ectopically expressed HuR rescues the epithelial barrier function in α4-silenced cells. (A) Representative immunoblots of claudin-1, claudin-3, ZO-1, and E-cadherin in α4-deficient cells with or without HuR overexpression. The cell lysates were harvested 48 h after the cells were transfected with C-siRNA or cotransfected with siα4 and recombinant adenoviral plasmids containing HuR (AdHuR) or control adenoviral vector (Adnull). (B) Changes in the epithelial barrier function as indicated by changes in TEER and FITC-dextran paracellular permeability in the cells shown in panel A. The values are the means and SEM of data from six samples. *, $P < 0.05$ compared with C-siRNA-transfected cells or cells cotransfected with siα4 and AdHuR.

involves IκB kinase α (IKKα) or protein kinase Cα (PKCα) (28, 29), we examined changes in phosphorylation of IKKα and PKCα after α4 silencing in cultured IECs. As shown in Fig. 6C, inhibition of α4 by transfection with siα4 markedly increased the levels of phosphorylated IKKα (p-IKKα) without altering total IKKα abundance, while the levels of phosphorylated PKCα did not change significantly (data not shown). Importantly, inhibition of IKKα activity following treatment with a specific IKKα inhibitor, BAY11-7082, prevented the suppression of HuR induced by α4 silencing and restored normal cellular HuR levels (Fig. 6C). Moreover, inhibition of the proteasome by MG132 also enhanced HuR levels in α4-deficient cells (Fig. 6D). Additionally, treatments with BAY11-7082 or MG132 did not affect cell viability, as measured by trypan blue staining (data not shown). We also examined the effect of α4 silencing on the stability of the full-length HuR-TAP (where TAP represents the tandem affinity purification tag) carrying each of the resulting point mutations, including pTAP-HuR3A (carrying three nonphosphorylatable mutations, S88A, S100A, and T118A), pTAP-HuR3D (carrying three nonphosphorylatable mutations, S88D, S100D, and T118D), and pTAP-HuR K182R, as described previously (28, 30). As shown in Fig. S6 in the supplemental material, in each transfection group, both the HuR wild type (WT)-TAP and the endogenous HuR were labile after α4 silencing. In addition, each of the HuR-TAP point mutants was also labile, indicating that all the mutated sites we tested are unrelated to α4 silencing-mediated HuR degradation.

Taken together, our findings suggest that α4 enhances HuR stability by repressing IKKα-mediated HuR phosphorylation (Fig. 6E). This process is carried out through the interaction of α4 with IKKα, which inhibits the degradation of the HuR protein by reducing its ubiquitination. In contrast, decreasing the levels of α4 destabilizes HuR by enhancing IKKα-dependent HuR phosphorylation and subsequent ubiquitin-mediated proteolysis, leading to reduced expression of various IJ proteins and dysfunction of the epithelial barrier.

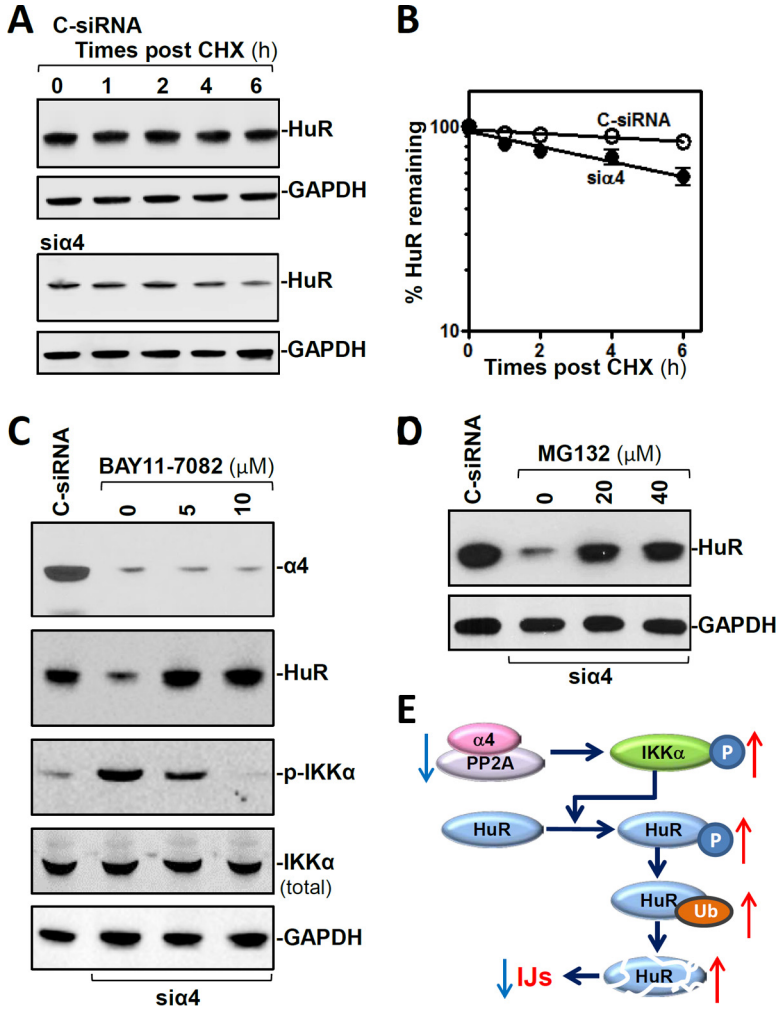

FIG 6 α4 silencing enhances HuR degradation by inducing IKKα-dependent phosphorylation. (A) Half-life of HuR protein after transfection with C-siRNA (top) or siα4 (bottom). The cells were exposed to CHX (10 μg/ml) 48 h after the transfection, and levels of HuR and the loading control GAPDH were examined at different times after the administration of CHX. (B) Percent HuR protein remaining in the cells shown in panel A. The values are the means ± SEM of data from three samples. (C) Immunoblots of HuR and phosphorylated and total IKKα in α4-deficient IECs treated with a specific IKKα inhibitor, BAY11-7082. Twenty-four hours after the cells were transfected with siα4, different concentrations of BAY11-7082 were added to the medium. The cell lysates were harvested 24 h after exposure to BAY11-7082. (D) Immunoblots of HuR in α4-deficient IECs treated with the proteasome inhibitor MG132 for 24 h. (E) Model proposed to explain the influence of α4 upon HuR degradation. In the model, decreasing the levels of α4/PP2A complex increased HuR degradation by enhancing IKKα-dependent HuR phosphorylation and subsequent ubiquitin (Ub)-mediated proteolysis. Decreased HuR led to inhibition of the expression of IJ proteins and epithelial barrier dysfunction.

DISCUSSION

Disruption of human intestinal mucosal homeostasis and epithelial integrity has serious pathological consequences, especially in patients supported with total parenteral nutrition (7, 31). Understanding the underlying mechanisms and developing successful medical treatments to maintain the integrity of the intestinal epithelium in patients with critical illness remains a major and urgent challenge. Using a conditional gene-targeting approach specific for the intestinal epithelium, we show here that the PP2A-associated protein α4 is essential for mucosal maturation and for maintaining epithelial homeostasis and barrier function. Targeted deletion of α4 in IECs resulted in striking defects in the mucosal morphology of the small intestine, as evidenced by significant crypt enlargement and villus shrinkage, along with defective differentiation and mislocalization of Paneth cells. The α4-deficient intestinal epithelium also exhibited

increased gut permeability in mice. Experiments aimed at characterizing α4 targets in this process suggested that the inhibition of IJ expression and subsequent gut barrier dysfunction induced by α4 deletion resulted primarily from a decrease in the abundance of cellular HuR. These findings advance our understanding of the physiological function of α4 in the intestinal epithelium and highlight a novel role of α4 deficiency in the pathogenesis of gut barrier dysfunction under various pathological conditions.

The results reported here provide the first demonstration that α4 functions as an important biological regulator that coordinates the maturation, homeostasis, and barrier function of the intestinal epithelium. As shown, α4 was highly expressed in the intestinal epithelium, and its cellular levels increased in migrating IECs after wounding but decreased in the intestinal mucosal tissues with erosion/inflammation in patients with IBD. Mouse genetic studies have demonstrated that the α4-deficient epithelium of the small intestine displayed the increased crypt expansion that was associated with a gross abnormality in polarity machineries. α4 loss also caused Paneth cell mislocalization, reduced IEC migration along the crypt-villus axis, and increased apoptosis in the intestinal epithelium. These results reveal that α4 slows down the regeneration of the intestinal mucosa and is essential for the maturation and homeostasis of the intestinal epithelium. Consistent with our findings, overexpression of α4 protects cells from a variety of stress stimuli, such as DNA damage and nutrient limitation (11), whereas α4 silencing inhibits cell spreading and migration in fibroblasts (13). However, opposing evidence also exists supporting a proproliferative influence of α4, primarily in studies conducted in cultured cells. For example, cell proliferation is stimulated by ectopic α4 overexpression in several lines of cancer cells but is inhibited by α4 silencing (12, 32). Thus, it appears that α4 can act as a proproliferative or antiproliferative factor, likely depending on the cell type, the presence of other factors, and the growth conditions.

Our results also indicate that α4 deletion in IECs disrupts the epithelial barrier function predominantly by decreasing the cellular levels of HuR. HuR has been shown to play an important role in the posttranscriptional control of mRNAs bearing U- and AU-rich elements (33) and is crucial for maintaining intestinal epithelium homeostasis and integrity (5, 20, 34, 35). We have reported that HuR promotes the translation and stability of mRNAs encoding various IJs and enhances the function of the epithelial barrier in both *in vitro* and *in vivo* models (26, 36). The targeted deletion of HuR in IECs delays the recovery of the intestinal barrier function after exposure to mesenteric ischemia/reperfusion in mice (27). In addition, it was reported that HuR interacts with noncoding RNAs, such as microRNAs and long noncoding RNAs (lncRNAs), to jointly regulate the expression of HuR target mRNAs (23, 37). For example, HuR prevents lncRNA *H19*-induced gut barrier dysfunction by blocking miRNA-675 processing from *H19* (27), and HuR forms a complex with the lncRNA *SPRY4-IT1* to enhance TJ expression and epithelial barrier function synergistically (36). In the current study, the levels of HuR decreased specifically in the α4-deficient intestinal epithelium *in vivo* and in cultured IECs after α4 silencing. The reduction in HuR levels in cells with ablated α4 was associated with a decrease in the levels of TJ claudin-1, claudin-3, ZO-1, and AJ E-cadherin and with increased paracellular permeability. Ectopically expressed HuR in α4-silenced IECs not only rescued the expression of these IJs, it also restored the barrier function to near normal. These findings demonstrate the importance of reduced levels of HuR in the pathogenesis of gut barrier dysfunction in IE-$\alpha4^{-/-}$ mice. However, HuR in the intestinal epithelium modulates distinct pathways of cell proliferation, migration, differentiation, and apoptosis (20–22, 37–39); HuR deletion also reduces tumor development by targeting multiple genes (35). The exact mechanisms whereby decreased HuR levels following α4 deletion delay mucosal maturation, as evidenced by crypt hyperplasia and villus shrinkage, defective differentiation of Paneth cells, and reduced migration, remain unknown and are being intensely investigated in our laboratory.

Although the mechanism by which α4 knockout lowers HuR abundance in the intestinal epithelium is unclear, the process involves the degradation of HuR and IKKα-dependent phosphorylation. In cultured IECs, α4 silencing by transfection with siα4 destabilized HuR protein but failed to alter the levels of *HuR* mRNA. Inhibition of

α4 also increased the levels of phosphorylated IKKα without affecting its total protein level. HuR is targeted for ubiquitination and undergoes ubiquitin-dependent degradation following heat shock in HeLa cells (28, 40); inhibition of proteasome activity elevates HuR levels in human diploid fibroblasts (38). HuR is phosphorylated by IKKα at S304, leading to HuR binding to the E3 ubiquitin ligase β-transducin repeat-containing protein for its degradation in response to metabolic stress (29), whereas HuR phosphorylation by checkpoint kinase 2 (CHEK2) enhances the resistance of HuR to proteasomal degradation (28). Recently, the tumor suppressor ECRG2 was shown to reduce cellular HuR levels by favoring ubiquitination of HuR at K182 for its degradation (39). Our results indicate that inhibition of either IKKα activity by BAY11-7082 or the proteasome by MG132 restored HuR levels in α4-silenced cells. These findings strongly support the notion that α4 regulates HuR degradation by altering IKKα-dependent HuR phosphorylation and subsequent ubiquitin-mediated proteolysis. Clearly, more studies are needed to determine how α4/PP2A association modulates IKKα activity and to further define the molecular process by which HuR is ubiquitinated and degraded after α4 silencing.

In summary, our results indicate that α4 regulates the proliferation, migration, apoptosis, polarity, and differentiation of IECs in mice. Normal expression of α4 is required for intestinal mucosal maturation and for maintaining epithelial homeostasis and barrier function. As the physiological role of α4 in the intestinal epithelium comes into focus, we propose that transient changes in cellular α4 are an important adaptive mechanism whereby the mammalian intestinal epithelium preserves its homeostasis and integrity in response to stressful environments and pathologies. These findings suggest that α4 is a promising therapeutic target for interventions to protect epithelial integrity and barrier function in patients with critical surgical illness.

MATERIALS AND METHODS

Chemicals and cell culture. Disposable cultureware was purchased from Corning Glass Works (Corning, NY). Tissue culture media, Lipofectamine 2000, and dialyzed fetal bovine serum (dFBS) were obtained from Invitrogen (Carlsbad, CA), and chemicals were obtained from Sigma (St. Louis, MO). Antibodies recognizing α4, PP2A, β-PIX, Rac1, claudin-1, claudin-3, ZO-1, occludin, E-cadherin, HuR, CUGBP1, total and p-IKKα, and GAPDH (glyceraldehyde-3-phosphate dehydrogenase) were purchased from Cell Signaling Technologies (Danvers, MA) and Santa Cruz Biotechnology (Santa Cruz, CA). A secondary antibody conjugated to horseradish peroxidase was purchased from Sigma. The IEC-6 cell line was purchased from the American Type Culture Collection (ATCC) at passage 13. Stock cells were maintained in T-150 flasks in Dulbecco's modified Eagle medium (DMEM) supplemented with 5% heat-inactivated FBS, 10 μg/ml insulin, and 50 μg/ml gentamicin sulfate. The flasks were incubated at 37°C in a humidified atmosphere of 90% air and 10% CO_2, and passages 15 to 20 were used in the experiments. Stable Cdx2-transfected IECs (IEC-Cdx2L1) were developed from IEC-6 cells and maintained as described previously (41). Before experiments, IEC-Cdx2L1 cells were grown in DMEM containing 4 mM IPTG (isopropyl-β-D-thiogalactopyranoside) for 16 days to induce cell differentiation, as described previously (42). Caco-2 cells were purchased from ATCC and maintained under standard culture conditions, as described previously (43).

Generation of IE-α4$^{-/-}$ mice. The strategy to generate and genotype mice with intestinal epithelium-specific α4 deletion (IE-α4$^{-/-}$ mice) by using the Vil-Cre-loxP-mediated gene deletion approach is provided in Fig. S1 in the supplemental material. The frozen embryos of α4$^{fl/fl}$ mice were kindly provided by Nobuo Sakaguchi (Kumamoto University School of Medicine, Kumamoto, Japan) (24). After recovery of α4$^{fl/fl}$ frozen embryos, α4$^{fl/fl}$ mice were crossed with mice carrying Vil-Cre (Jackson Laboratory; SN 004586). Heterozygous IE-α4$^{+/-}$ mice appeared phenotypically normal and were subsequently intercrossed for the generation of homozygous IE-α4$^{-/-}$ (α4$^{fl/fl}$-Vil-Cre^{+}) mice. α4$^{fl/fl}$-Vil-Cre^{-} mice served as littermate controls. Age-matched littermate and IE-α4$^{-/-}$ mice were used for phenotype analysis, and the levels of *α4* mRNA and protein in the small intestinal mucosa were also examined in each group of experiments.

Animal experiments. All experiments were approved by the animal experimental ethics committee guidelines of the University of Maryland Baltimore Institutional Animal Care and Use Committee and Baltimore VA hospital. Control littermate and IE-α4$^{-/-}$ mice were housed and handled within a specific-pathogen-free breeding barrier and cared for by trained technicians and veterinarians. The mice were allowed free access to food and tap water. To examine gut mucosal growth, BrdU was incorporated into the intestinal mucosa by intraperitoneal (i.p.) injection of 1 mg BrdU (Sigma, St. Louis, MO) in phosphate-buffered saline (44). The animals were euthanized by CO_2 asphyxiation. Four-centimeter small intestinal segments that were 0.5 cm distal to the ligament of Trietz were collected 30 min after injection. To chase epithelial cell migration along the crypt-villus axis, the small intestinal mucosa was harvested at different times after BrdU injection. The mucosa was scraped from the underlying smooth muscle with a glass microscope slide and used for measurement of the levels of various mRNAs and protein expression.

Histological analysis. Dissected and opened intestines were mounted onto a solid surface and fixed in formalin and paraffin. Sections (5 μm thick) were stained with hematoxylin and eosin (H&E) for general histology. Analysis was blinded; the slides were coded and were only decoded after examination. By using a microscope eyepiece reticle, the overall length of villus and crypts of each section was measured, and the villus/crypt ratio was calculated. Microscopic damage in the intestinal mucosa was measured and semiquantified as described previously (22).

Assays of gut permeability in mice. FITC-conjugated dextran dissolved in water (Sigma; 4KD; 600 mg/kg of body weight) was administered to mice via gavage as described previously (36, 45). Blood was collected 4 h thereafter via cardiac puncture. The concentration of FITC-dextran in serum was determined using a plate reader with an excitation wavelength at 490 nm and an emission wavelength of 530 nm. The concentration of FITC-dextran in sera was determined by comparison to the FITC-dextran standard curve.

Construction of overexpression vectors and RNA interference. Recombinant adenoviral vectors expressing human HuR (AdHuR) were constructed by using the Adeno-X expression system (Clontech) (37). Briefly, the full-length cDNA of human wild-type HuR was cloned into the pShuttle vector by BamHI/HindIII digestion and ligating the resultant fragments into the XbaI site of the pShuttle vector. pAdeno-HuR (AdHuR) was constructed by digesting the pShuttle construct with PI-SceI/I-CeuI and ligating the resultant fragment into the PI-SceI/I-CeuI sites of the pAdeno-X adenoviral vector. Recombinant adenoviral plasmids were packaged into infectious adenoviral particles by transfecting HEK-293 human embryonic kidney cells; titers of the adenoviral stock were determined by standard plaque-forming assay. pAdeno-X, a replication-incompetent adenovirus carrying no HuR cDNA insert (Adnull), was grown and purified as described above and served as a control adenovirus. Cells were infected with AdHuR or Adnull, and expression of HuR was assayed 24 or 48 h after the infection.

Expression of α4 in cultured IECs was silenced by transfection with specific small interfering RNA, as described previously (11); siα4 and C-siRNA were purchased from Santa Cruz Biotechnology. For each 60-mm cell culture dish, 15 μl of the 20 μM stock duplex siα4 or C-siRNA was used. Forty-eight hours after transfection using Lipofectamine, cells were harvested for analysis.

Western blot analysis. Whole-cell lysates were prepared using 2% SDS, sonicated, and centrifuged at 4°C for 15 min. The supernatants were boiled and size fractionated by SDS-PAGE. After the blots were incubated with primary antibody and secondary antibodies, immunocomplexes were developed by using chemiluminescence.

RT followed by conventional PCR analysis and real-time Q-PCR analysis. Total RNA was isolated using an RNeasy minikit (Qiagen, Valencia, CA) and used in reverse transcription (RT) and PCR amplification reactions as described previously (46). The levels of *Gapdh* PCR product were assessed to monitor the evenness of RNA input in RT-PCR samples. RT-quantitative (Q)-PCR analysis was performed using 7500-Fast real-time PCR systems with specific primers, probes, and software (Applied Biosystems, Foster City, CA).

Statistics. All values are expressed as means and standard errors of the mean (SEM). An unpaired, two-tailed Student *t* test was used where indicated, with *P* values of <0.05 considered significant. When assessing multiple groups, one-way analysis of variance (ANOVA) was utilized, with Tukey's *post hoc* test (47). The statistical software used was SPSS17.1.

SUPPLEMENTAL MATERIAL

Supplemental material for this article may be found at https://doi.org/10.1128/MCB.00631-17.

SUPPLEMENTAL FILE 1, PDF file, 0.7 MB.

ACKNOWLEDGMENTS

This work was supported by Merit Review Awards (to J.-Y.W., D.J.T., and J.N.R.) from the U.S. Department of Veterans Affairs, grants from the National Institutes of Health (DK57819, DK61972, and DK68491 to J.-Y.W.), and funding from the National Institute on Aging-Intramural Research Program, NIH (to M.G.). J.-Y.W. is a Senior Research Career Scientist, Biomedical Laboratory Research and Development Service, U.S. Department of Veterans Affairs.

H.K.C. performed most experiments and summarized data. S.R.W., L.X., and N.R. performed experiments *in vivo* and histochemical staining. D.J.T. performed experiments related to human samples. P.Y. contributed to the generation of the mouse model. M.G. contributed to experimental design and data analysis. J.N.R. and J.-Y.W. designed experiments, analyzed data, and prepared figures; J.-Y.W. drafted the manuscript.

We have no conflicts to disclose.

REFERENCES

1. Clevers H. 2013. The intestinal crypt, a prototype stem cell compartment. Cell 154:274–284. https://doi.org/10.1016/j.cell.2013.07.004.
2. Xiao L, Wang JY. 2014. RNA-binding proteins and microRNAs in gastrointestinal epithelial homeostasis and diseases. Curr Opin Pharmacol 19:46–53. https://doi.org/10.1016/j.coph.2014.07.006.
3. Delgado ME, Grabinger T, Brunner T. 2016. Cell death at the intestinal

epithelial front line. FEBS J 283:2701–2719. https://doi.org/10.1111/febs.13575.
4. Xiao L, Wu J, Wang JY, Chung HK, Kalakonda S, Rao JN, Gorospe M, Wang JY. 2018. Long noncoding RNA uc.173 promotes renewal of the intestinal mucosa by inducing degradation of microRNA 195. Gastroenterology 154:599–611. https://doi.org/10.1053/j.gastro.2017.10.009.
5. Liu L, Zhuang R, Xiao L, Chung HK, Luo J, Turner DJ, Rao JN, Gorospe M, Wang JY. 2017. HuR enhances early restitution of the intestinal epithelium by increasing Cdc42 translation. Mol Cell Biol 37:e00574-16. https://doi.org/10.1128/MCB.00574-16.
6. Freeman JJ, Feng Y, Demehri FR, Dempsey PJ, Teitelbaum DH. 2015. TPN-associated intestinal epithelial cell atrophy is modulated by TLR4/EGF signaling pathways. FASEB J 29:2943–2958. https://doi.org/10.1096/fj.14-269480.
7. Mittal R, Coopersmith CM. 2014. Redefining the gut as the motor of critical illness. Trends Mol Med 20:214–223. https://doi.org/10.1016/j.molmed.2013.08.004.
8. Inui S, Kuwahara K, Mizutani J, Maeda K, Kawai T, Nakayasu H, Sakaguchi N. 1995. Molecular cloning of a cDNA clone encoding a phosphoprotein component related to the Ig receptor-mediated signal transduction. J Immunol 154:2714–2723.
9. Kong M, Fox CJ, Mu J, Solt L, Xu A, Cinalli RM, Birnbaum MJ, Lindsten T, Thompson CB. 2004. The PP2A-associated protein alpha4 is an essential inhibitor of apoptosis. Science 306:695–698. https://doi.org/10.1126/science.1100537.
10. LeNoue-Newton ML, Wadzinski BE, Spiller BW. 2016. The three type 2A protein phosphatases, PP2Ac, PP4c and PP6c, are differentially regulated by Alpha4. Biochem Biophys Res Commun 475:64–69. https://doi.org/10.1016/j.bbrc.2016.05.036.
11. Kong M, Ditsworth D, Lindsten T, Thompson CB. 2009. α4 is an essential regulator of PP2A phosphatase activity. Mol Cell 36:51–60. https://doi.org/10.1016/j.molcel.2009.09.025.
12. Chen LP, Lai YD, Li DC, Zhu XN, Yang P, Li WX, Zhu W, Zhao J, Li XD, Xiao YM, Zhang Y, Xing XM, Wang Q, Zhang B, Lin YC, Zeng JL, Zhang SX, Liu CX, Li ZF, Zeng XW, Lin ZN, Zhuang ZX, Chen W. 2011. α4 is highly expressed in carcinogen-transformed human cells and primary human cancers. Oncogene 30:2943–2953. https://doi.org/10.1038/onc.2011.20.
13. Kong M, Bui TV, Ditsworth D, Gruber JJ, Goncharov D, Krymskaya VP, Lindsten T, Thompson CB. 2007. The PP2A-associated protein α4 plays a critical role in the regulation of cell spreading and migration. J Biol Chem 282:29712–29720. https://doi.org/10.1074/jbc.M703159200.
14. Janssens V, Goris J. 2001. Protein phosphatase 2A: a highly regulated family of serine/threonine phosphatases implicated in cell growth and signalling. Biochem J 353:417–439.
15. Du H, Huang Y, Zaghlula M, Walters E, Cox TC, Massiah MA. 2013. The MID1 E3 ligase catalyzes the polyubiquitination of Alpha4 (α4), a regulatory subunit of protein phosphatase 2A (PP2A): novel insights into MID1-mediated regulation of PP2A. J Biol Chem 288:21341–21350. https://doi.org/10.1074/jbc.M113.481093.
16. Wang JY, Xiao L, Wang JY. 2017. Posttranscriptional regulation of intestinal epithelial integrity by noncoding RNAs. Wiley Interdiscip Rev RNA 8. https://doi.org/10.1002/wrna.1399.
17. Melendez J, Grogg M, Zheng Y. 2011. Signaling role of Cdc42 in regulating mammalian physiology. J Biol Chem 286:2375–2381. https://doi.org/10.1074/jbc.R110.200329.
18. Erickson JW, Cerione RA. 2001. Multiple roles for Cdc42 in cell regulation. Curr Opin Cell Biol 13:153–157. https://doi.org/10.1016/S0955-0674(00)00192-7.
19. Melendez J, Liu M, Sampson L, Akunuru S, Han X, Vallance J, Witte D, Shroyer N, Zheng Y. 2013. Cdc42 coordinates proliferation, polarity, migration, and differentiation of small intestinal epithelial cells in mice. Gastroenterology 145:808–819. https://doi.org/10.1053/j.gastro.2013.06.021.
20. Liu L, Ouyang M, Rao JN, Zou T, Xiao L, Chung HK, Wu J, Donahue JM, Gorospe M, Wang JY. 2015. Competition between RNA-binding proteins CELF1 and HuR modulates MYC translation and intestinal epithelium renewal. Mol Biol Cell 26:1797–1810. https://doi.org/10.1091/mbc.E14-11-1500.
21. Liu L, Christodoulou-Vafeiadou E, Rao JN, Zou T, Xiao L, Chung HK, Yang H, Gorospe M, Kontoyiannis D, Wang JY. 2014. RNA-binding protein HuR promotes growth of small intestinal mucosa by activating the Wnt signaling pathway. Mol Biol Cell 25:3308–3318. https://doi.org/10.1091/mbc.E14-03-0853.
22. Chung HK, Chen Y, Rao JN, Liu L, Xiao L, Turner DJ, Yang P, Gorospe M, Wang JY. 2015. Transgenic expression of miR-222 disrupts intestinal epithelial regeneration by targeting multiple genes including Frizzled-7. Mol Med 21:676–687. https://doi.org/10.2119/molmed.2015.00147.
23. Zhuang R, Rao JN, Zou T, Liu L, Xiao L, Cao S, Hansraj NZ, Gorospe M, Wang JY. 2013. miR-195 competes with HuR to modulate stim1 mRNA stability and regulate cell migration. Nucleic Acids Res 41:7905–7919. https://doi.org/10.1093/nar/gkt565.
24. Yamashita T, Inui S, Maeda K, Hua DR, Takagi K, Fukunaga K, Sakaguchi N. 2006. Regulation of CaMKII by α4/PP2Ac contributes to learning and memory. Brain Res 1082:1–10. https://doi.org/10.1016/j.brainres.2006.01.101.
25. Mukherjee N, Corcoran DL, Nusbaum JD, Reid DW, Georgiev S, Hafner M, Ascano M, Jr, Tuschl T, Ohler U, Keene JD. 2011. Integrative regulatory mapping indicates that the RNA-binding protein HuR couples pre-mRNA processing and mRNA stability. Mol Cell 43:327–339. https://doi.org/10.1016/j.molcel.2011.06.007.
26. Yu TX, Wang PY, Rao JN, Zou T, Liu L, Xiao L, Gorospe M, Wang JY. 2011. Chk2-dependent HuR phosphorylation regulates occludin mRNA translation and epithelial barrier function. Nucleic Acids Res 39:8472–8487. https://doi.org/10.1093/nar/gkr567.
27. Zou T, Jaladanki SK, Liu L, Xiao L, Chung HK, Wang JY, Xu Y, Gorospe M, Wang JY. 2016. H19 long noncoding RNA regulates intestinal epithelial barrier function via microRNA 675 by interacting with RNA-binding protein HuR. Mol Cell Biol 36:1332–1341. https://doi.org/10.1128/MCB.01030-15.
28. Abdelmohsen K, Srikantan S, Yang X, Lal A, Kim HH, Kuwano Y, Galban S, Becker KG, Kamara D, de Cabo R, Gorospe M. 2009. Ubiquitin-mediated proteolysis of HuR by heat shock. EMBO J 28:1271–1282. https://doi.org/10.1038/emboj.2009.67.
29. Chu PC, Chuang HC, Kulp SK, Chen CS. 2012. The mRNA-stabilizing factor HuR protein is targeted by β-TrCP protein for degradation in response to glycolysis inhibition. J Biol Chem 287:43639–43650. https://doi.org/10.1074/jbc.M112.393678.
30. Masuda K, Abdelmohsen K, Kim MM, Srikantan S, Lee EK, Tominaga K, Selimyan R, Martindale JL, Yang X, Lehrmann E, Zhang Y, Bexker KG, Wang JY, Kim HH, Gorospe M. 2011. Global dissociation of HuR-mRNA complexes promotes cell survival after ionizing radiation. EMBO J 30:1040–1053. https://doi.org/10.1038/emboj.2011.24.
31. Lindemans CA, Calafiore M, Mertelsmann AM, O'Connor MH, Dudakov JA, Jenq RR, Velardi E, Young LF, Smith OM, Lawrence G, Ivanov JA, Fu YY, Takashima S, Hua G, Martin ML, O'Rourke KP, Lo YH, Mokry M, Romera-Hernandez M, Cupedo T, Dow L, Nieuwenhuis EE, Shroyer NF, Liu C, Kolesnick R, van den Brink MRM, Hanash AM. 2015. Interleukin-22 promotes intestinal-stem-cell-mediated epithelial regeneration. Nature 528:560–564. https://doi.org/10.1038/nature16460.
32. Liu J, Cai M, Chen J, Liao Y, Mai S, Li Y, Huang X, Liu Y, Zhang J, Kung H, Zeng Y, Zhou F, Xie D. 2014. α4 contributes to bladder urothelial carcinoma cell invasion and/or metastasis via regulation of E-cadherin and is a predictor of outcome in bladder urothelial carcinoma patients. Eur J Cancer 50:840–851. https://doi.org/10.1016/j.ejca.2013.11.038.
33. Simone LE, Keene JD. 2013. Mechanisms coordinating ELAV/Hu mRNA regulons. Curr Opin Genet Dev 23:35–43. https://doi.org/10.1016/j.gde.2012.12.006.
34. Yu TX, Rao JN, Zou T, Liu L, Xiao L, Ouyang M, Cao S, Gorospe M, Wang JY. 2013. Competitive binding of CUGBP1 and HuR to occludin mRNA controls its translation and modulates epithelial barrier function. Mol Biol Cell 24:85–99. https://doi.org/10.1091/mbc.E12-07-0531.
35. Giammanco A, Blanc V, Montenegro G, Klos C, Xie Y, Kennedy S, Luo J, Chang SH, Hla T, Nalbantoglu I, Dharmarajan S, Davidson NO. 2014. Intestinal epithelial HuR modulates distinct pathways of proliferation and apoptosis and attenuates small intestinal and colonic tumor development. Cancer Res 74:5322–5335. https://doi.org/10.1158/0008-5472.CAN-14-0726.
36. Xiao L, Rao JN, Cao S, Liu L, Chung HK, Zhang Y, Zhang J, Liu Y, Gorospe M, Wang JY. 2016. Long noncoding RNA SPRY4-IT1 regulates intestinal epithelial barrier function by modulating the expression levels of tight junction proteins. Mol Biol Cell 27:617–626. https://doi.org/10.1091/mbc.E15-10-0703.
37. Zou T, Rao JN, Liu L, Xiao L, Yu TX, Jiang P, Gorospe M, Wang JY. 2010. Polyamines regulate the stability of JunD mRNA by modulating the competitive binding of its 3′ untranslated region to HuR and AUF1. Mol Cell Biol 30:5021–5032. https://doi.org/10.1128/MCB.00807-10.
38. Bonelli MA, Alfieri RR, Desenzani S, Petronini PG, Borghetti AF. 2004. Proteasome inhibition increases HuR level, restores heat-inducible

HSP72 expression and thermotolerance in WI-38 senescent human fibroblasts. Exp Gerontol 39:423–432. https://doi.org/10.1016/j.exger.2003.12.004.
39. Lucchesi C, Sheikh MS, Huang Y. 2016. Negative regulation of RNA-binding protein HuR by tumor-suppressor ECRG2. Oncogene 35:2565–2573. https://doi.org/10.1038/onc.2015.339.
40. Grammatikakis I, Abdelmohsen K, Gorospe M. 2017. Posttranslational control of HuR function. Wiley Interdiscip Rev RNA 8. https://doi.org/10.1002/wrna.1372.
41. Zhang Y, Zhang Y, Xiao L, Yu TX, Li JZ, Rao JN, Turner DJ, Gorospe M, Wang JY. 2017. Cooperative repression of insulin-like growth factor type 2 receptor translation by microRNA 195 and RNA-binding protein CUGBP1. Mol Cell Biol 37:e00225-17. https://doi.org/10.1128/MCB.00225-17.
42. Rao JN, Platoshyn O, Li L, Guo X, Golovina VA, Yuan JX, Wang JY. 2002. Activation of K^+ channels and increased migration of differentiated intestinal epithelial cells after wounding. Am J Physiol Cell Physiol 282:C885–C898. https://doi.org/10.1152/ajpcell.00361.2001.
43. Zou T, Rao JN, Liu L, Xiao L, Chung HK, Li Y, Chen G, Gorospe M, Wang JY. 2015. JunD enhances miR-29b levels transcriptionally and posttranscriptionally to inhibit proliferation of intestinal epithelial cells. Am J Physiol Cell Physiol 308:C813–C824. https://doi.org/10.1152/ajpcell.00027.2015.
44. Chung HK, Rao JN, Zou T, Liu L, Xiao L, Gu H, Turner DJ, Yang P, Wang JY. 2014. Jnk2 deletion disrupts intestinal mucosal homeostasis and maturation by differentially modulating RNA-binding proteins HuR and CUGBP1. Am J Physiol Cell Physiol 306:C1167–C1175. https://doi.org/10.1152/ajpcell.00093.2014.
45. Hubbard WJ, Choudhry M, Schwacha MG, Kerby JD, Rue LW III, Bland KI, Chaudry IH. 2005. Cecal ligation and puncture. Shock 24(Suppl 1):S52–S57. https://doi.org/10.1097/01.shk.0000191414.94461.7e.
46. Cao S, Xiao L, Rao JN, Zou T, Liu L, Zhang D, Turner DJ, Gorospe M, Wang JY. 2014. Inhibition of Smurf2 translation by miR-322/503 modulates TGF-beta/Smad2 signaling and intestinal epithelial homeostasis. Mol Biol Cell 25:1234–1243. https://doi.org/10.1091/mbc.E13-09-0560.
47. Harter HL. 1960. Critical values for Duncan's new multiple range test. Biometrics 16:671–685. https://doi.org/10.2307/2527770.